

# We are IntechOpen, the world's leading publisher of Open Access books Built by scientists, for scientists

6,900

Open access books available

186,000

International authors and editors

200M

Downloads

Our authors are among the

154

Countries delivered to

TOP 1%

most cited scientists

12.2%

Contributors from top 500 universities



WEB OF SCIENCE™

Selection of our books indexed in the Book Citation Index  
in Web of Science™ Core Collection (BKCI)

Interested in publishing with us?  
Contact [book.department@intechopen.com](mailto:book.department@intechopen.com)

Numbers displayed above are based on latest data collected.  
For more information visit [www.intechopen.com](http://www.intechopen.com)



---

# Thin Film Solar Cells Using Earth-Abundant Materials

---

Parag S. Vasekar and Tara P. Dhakal

Additional information is available at the end of the chapter

<http://dx.doi.org/10.5772/51734>

---

## 1. Introduction

In a p-n junction photovoltaic (PV) cell, a photon of light produces an electron hole pair if the energy of the photon is at least equal to the band gap of the material constituting the p-n junction. The electrons and holes first diffuse toward the respective edge of the depletion region, and then drift across the junction due to the built-in potential and are collected at the electrodes. Thus, materials with long minority carrier life times and high carrier mobilities are desired for high efficiency. Because electrons have higher mobility than the holes, a p-type semiconductor is used as light absorber in a p-n junction solar cell.

The theoretical efficiency limit for an ideal homo-junction solar cell as calculated by Loferski [1] is 23%, and this maximum efficiency falls in the vicinity of the absorbers with band gap energy of 1.5 eV. A more justifiable theoretical efficiency limit that used atomic processes was put forward by Shockley and Queisser [2] later in the sixties. According to this theoretical efficiency limit, also known as the Shockley-Queisser limit, a maximum efficiency of 30% for a band gap of 1.1 eV is possible (assuming only radiative recombination) if exposed to the sunlight of global air mass 1.5.

The most recent data published in *Progress in Photovoltaics* [3] depict an efficiency of 25% for a crystalline silicon (Si) solar cell measured under the global AM 1.5 spectrum at 25°C. This value of efficiency approaches the theoretical value set by Shockley-Queisser limit. However, coupled with its low absorption cross section and high synthesis and processing cost, this first generation crystalline Si- solar cell doesn't show promise for a low cost, thin film PV device.

For thin film technologies, amorphous silicon-hydrogen alloy (a-Si) solar cells have exhibited efficiencies in the 10-12% range [4] and are fabricated with low cost technology. However, degradation of the performance over time is a major issue associated with the a-Si solar cells. Recently, metal induced crystallization of a-Si is used to make thin film polycrystalline Si-solar cell at relatively low temperature in an effort to reduce the processing cost [5], but fabrication

of these devices is combined with high temperature chemical vapor deposition, which makes it incompatible with roll-to-roll processing. Other emerging second generation solar cells are thin film chalcogenides like CIGS ( $\text{CuInGaSe}_2$ ) and CdTe, which show terrestrial cell efficiency of 20.3% and 16.5% respectively [6,7]. The scarcity, cost and toxicity associated with In, Ga, and Cd elements present in these cells limit their sustainability in the future.

Thus wide spread applications of solar cells will require dramatic decrease in cost through the use of non-toxic, inexpensive, and earth-abundant materials. The drawbacks in the present PV materials motivate us to look for alternatives. Due to the low absorption cross section, crystalline silicon requires thick layers, which will increase costs. Amorphous silicon (a-Si) has a higher absorption cross section and low processing cost compared to its crystalline counterpart, but it has stability problems. GaAs based solar cells have high efficiency, but the arsenic toxicity and the substrate cost limit their use. CIGS thin film solar cells show promise if the scarce and costly indium and gallium could be replaced by other elements. The quaternary compound semiconductor CZTS ( $\text{Cu}_2\text{ZnSnS}_4$ ) [8] possesses promising characteristic optical properties; band-gap energy of about 1.5 eV and large absorption coefficient in the order of  $10^4 \text{ cm}^{-1}$ . The highly efficient CdTe solar cell is promising, but has obstacles such as cadmium toxicity, tellurium scarcity, and cost. While the results of research and commercialization of crystalline Si, GaAs, CIGS, CdTe, etc. cells are commendable, a search for alternative materials is indispensable and necessary to achieve low cost, light weight, and low toxicity arrays.

Property	CZTS	$\text{Zn}_3\text{P}_2$	$\text{FeS}_2$
Band gap	1.5 eV [10]	1.5 eV [11]	0.95 eV [12]
Absorption Coeff.	$\approx 10^4 \text{ cm}^{-1}$ [10]	$\approx 10^4 \text{ cm}^{-1}$ [13]	$3.3 \times 10^5 \text{ cm}^{-1}$ [12]
Electron diff. length	n/a <sup>†</sup>	4 to 10 $\mu\text{m}$ [11]	0.13 to 1 $\mu\text{m}$ [12]
Dark resistivity ( $\rho$ )	1 to $39 \times 10^3 \Omega \cdot \text{cm}$ [14]	$2.5 \times 10^3 \Omega \cdot \text{cm}$ [15]	$1.43 \Omega \cdot \text{cm}$ [16]
Carrier mobility ( $\mu$ )	$30 \text{ cm}^2/\text{Vs}$ [10]	$450 \text{ cm}^2/\text{Vs}$ [17]	200 to $300 \text{ cm}^2/\text{Vs}$ [12]

**Table 1.** Figure of Merits of CZTS,  $\text{Zn}_3\text{P}_2$  and  $\text{FeS}_2$  toward a PV cell compiled from the literature. <sup>†</sup>Although the exact value of the electron diffusion length of CZTS is not available, the quantum efficiency (QE) spectra suggest a relatively lower carrier diffusion length for this material.

In a recent study [9], a number of promising solar cell materials including CZTS,  $\text{Zn}_3\text{P}_2$ , and  $\text{FeS}_2$  etc. were identified as materials with low extraction cost. It is estimated that the cost of material extraction for CZTS,  $\text{Zn}_3\text{P}_2$  and  $\text{FeS}_2$  is around 0.005 cents/W, 0.0007 cents/W and 0.000002 cents/W respectively. More encouraging is the fact that the constituent materials of these absorbers are abundant in the earth's crust. The light absorption cross sections for CZTS,  $\text{Zn}_3\text{P}_2$  and  $\text{FeS}_2$  are all greater than  $10^4 \text{ cm}^{-1}$  (Table 1), thus making thin film devices practical. The band gaps are also in the optimum range for efficient photo-energy conversion. These three contenders will be discussed mainly in this review with some discussion on other earth-abundant candidates such as tin sulfide (SnS).

## 2. Copper zinc tin sulfide

### 2.1. Introduction

Thin film solar cells based on  $\text{Cu}(\text{In,Ga})(\text{S,Se})_2$  and  $\text{CdTe}$  have demonstrated significant improvement in the last few years, and they are also being transferred to production levels [18,19]. Out of these two technologies, CIGS based solar cells are the most efficient ones at the laboratory level and have demonstrated efficiencies in the range of 20% [6]. However, both CIGS and  $\text{CdTe}$  based thin film solar cells are hindered by potential environmental hazard issues [20] and scarcity issues associated with the constituent elements: mainly  $\text{Te}$ ,  $\text{In}$ ,  $\text{Ga}$ , and to some extent,  $\text{Se}$  [20,21]. Recent research trends are moving towards finding alternatives based on earth-abundant and non-toxic elements. An alternative material  $\text{Cu}(\text{Zn,Sn})(\text{S,Se})_2$  is being explored these days by the thin film photovoltaics community which contains earth-abundant materials like  $\text{Zn}$  and  $\text{Sn}$ . CZTS structure can be derived from  $\text{CuInS}_2$  chalcopyrite structure by replacing one-half of the constituent indium atoms by zinc and other half by tin. The resulting bandgap varies in the range of 0.8 eV for a selenide structure to 1.5 eV for a sulfide structure [22]. Copper-Zinc-Tin Sulfide or  $\text{Cu}_2\text{ZnSnS}_4$  (CZTS) has a nearly ideal direct bandgap (1.5 eV) to absorb the most of the visible solar spectrum as well as a high absorption coefficient ( $10^4 \text{ cm}^{-1}$ ). CZTS film contains neither rare metals nor toxic materials, and combined with the cadmium-free buffer layer, we can expect solar cells with complete non-toxicity.

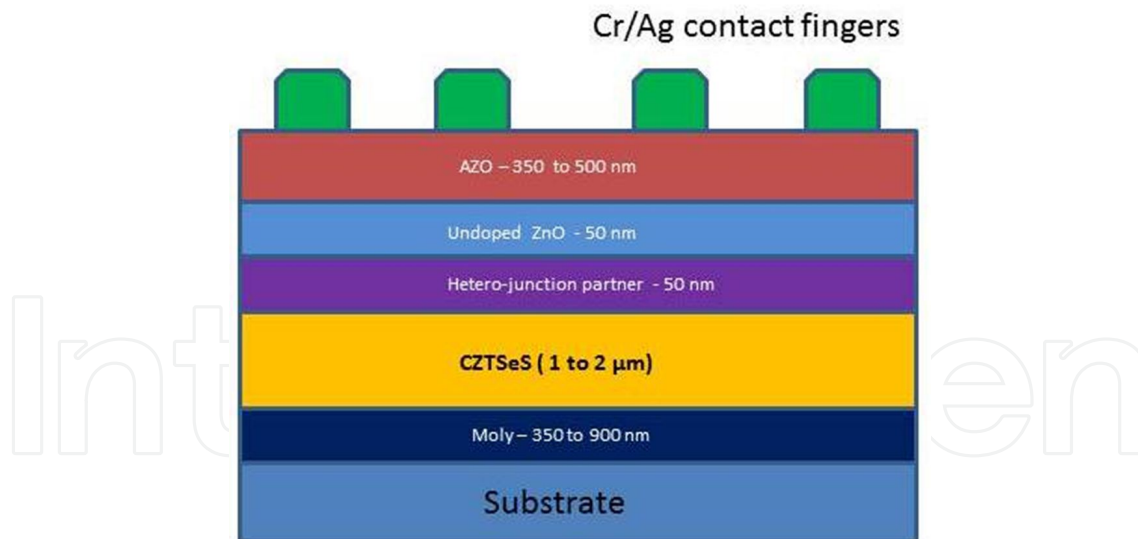


**Figure 1.** Schematic of the complete CZTSeS solar cell.

Several preparation methods have been reported in literature for preparation of CZTS solar cells [23]. These are physical vapor methods such as sulfurization of e-beam evaporated metallic layers and sputtered layers [24,25], RF magnetron sputtering [26], co-evaporation [27], hybrid sputtering [28]. Chemical methods involve sulfurization of electrochemically deposited metallic precursors [29], photochemical deposition [30], sol-gel sulfurization

methods [31], sol-gel spin-coated deposition [32] and spray pyrolysis [33,34]. In addition, there are syntheses based on solution methods [35,36].

Ever since Nakazawa reported the photovoltaic effect in a heterodiode of CZTS in 1988 [37], research in CZTS field has come a long way. The current highest efficiency for solution-processed CZTSeS based solar cells is 10.1% [38]. The efficiency for pure CZTS based solar cells that use the vacuum based approach is reported to be 8.4% [39]. The Schematic of a CZTSeS solar cell is as shown in Fig.1.

## 2.2. Crystal Structure

CIGSeS based films are mostly crystallized with a chalcopyrite structure [40], while CZTSeS based films exhibit either a Kesterite type of crystal structure or Stannite structure [41]. Because XRD peaks for Kesterite structure are similar to Stannite structure, it is difficult to distinguish between them unless other measurement techniques, such as neutron diffraction or Raman spectroscopy, are also employed. All three crystal structures are shown in Fig. 2 in order to understand the similarity and difference between them. It is also quite likely that both Kesterite and Stannite structures co-exist simultaneously because there is not much of energy difference for these structures to achieve/attain a stable state [41].

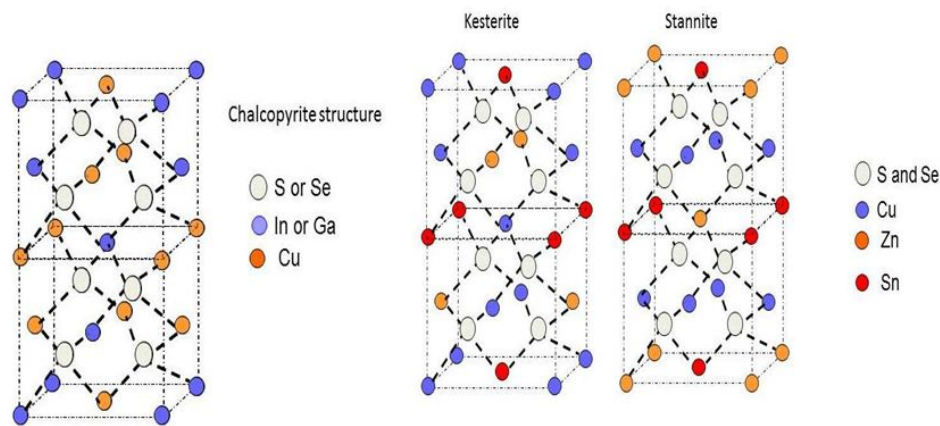


**Figure 2.** Chalcopyrite, Kesterite and Stannite crystal structures.

## 2.3. Electronic properties

The band-gap is the most important property of a photovoltaic material and near-optimum band-gap value around 1.5 eV is supposed to be ideal for effective photon absorption and photo-generation. CZTSe phase has a band-gap of 0.8 eV, while CZTS phase has a band-gap value of 1.5 eV [22]. The band-gap can be engineered between these two values by adding sulfur to CZTSe phase. The doping behavior in Kesterite is also controlled by intrinsic doping similar to their chalcopyrite counterparts. The p-type behavior of CZTSeS phase is controlled by  $\text{Cu}_{\text{Zn}}$  or  $\text{Cu}_{\text{Sn}}$  antisite donor defects, or this may also result due to direct creation of copper vacancy and compensation for  $\text{Zn}_{\text{Cu}}$  antisite and the S vacancy [41].

## 2.4. Phase stability

Similar to CIGSeS thin films, CZTSeS phase also has a narrow region of phase stability in which the device quality phase can be synthesized without any adverse effect of secondary phases. In fact, the phase stability region is even narrower as compared to chalcopyrites, thus making single phase device quality CZTSeS synthesis more difficult [42]. Solid state CZTS can also be synthesized through reactions between ZnS, Cu<sub>2</sub>S, and SnS<sub>2</sub>. As can be seen in the phase diagram in Fig. 3, there is very narrow region where CZTS is stable and secondary phases are very easy to form. Copper-poor and zinc-rich composition has been found to be ideal so far to obtain efficient devices from CZTS films [8].

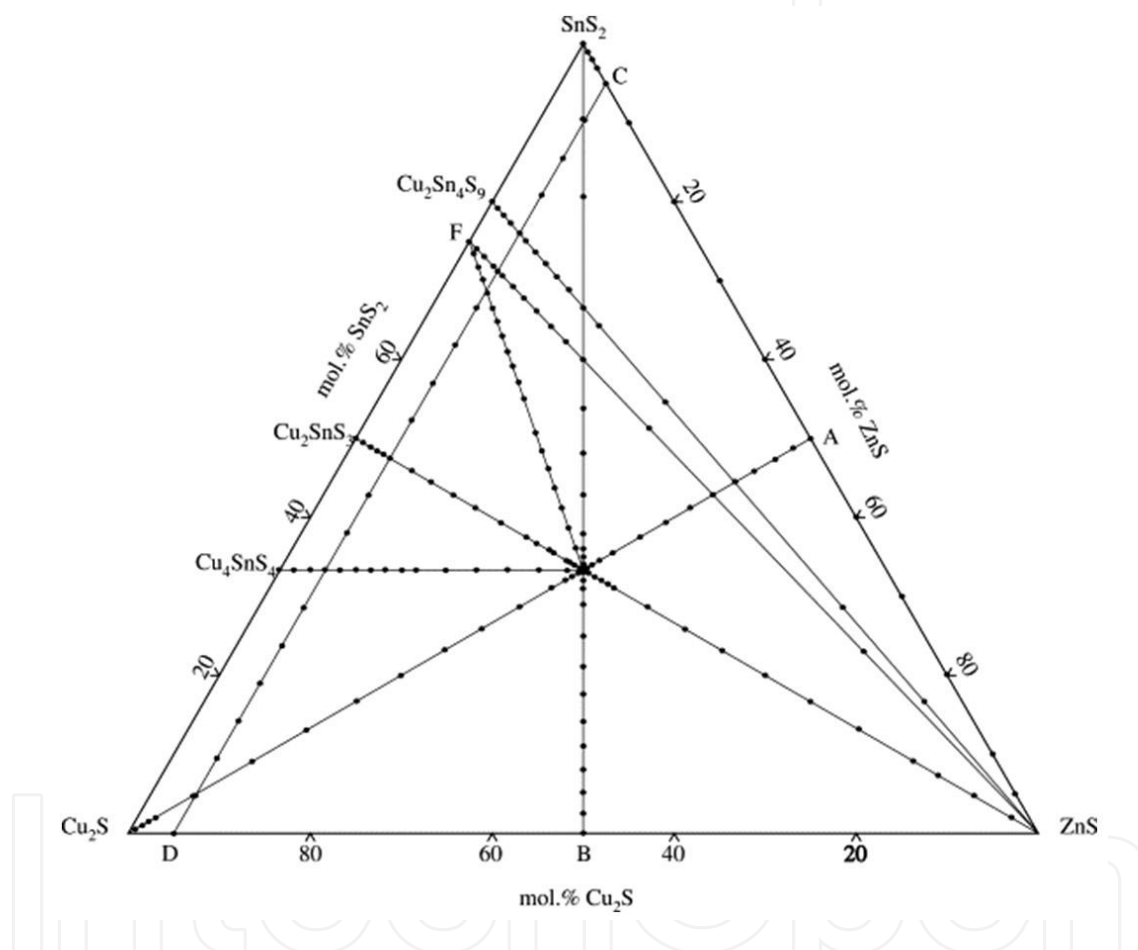


**Figure 3.** Ternary phase diagram of the Cu<sub>2</sub>S-ZnS-SnS<sub>2</sub> system. (Reprinted from [42] with permission from Elsevier).

## 2.5. Synthesis techniques

### 2.5.1. Vacuum based approaches ( sputtering/evaporation)

The synthesis techniques are both vacuum-based processes and non-vacuum based processes. Dr. Katagiri's group has pioneered vacuum-based approaches [8,22,24,43]. Their first report on E-B evaporated precursors followed by sulfurization yielded an efficiency of 0.66% [24]. With modification of fabrication process, the conversion efficiency was

gradually increased in their successive reports. It was observed that longer time and temperature cycles were detrimental for the performance of the CZTS films: hence, by adjusting the time and temperature cycles, Katagiri et al reported an efficiency of 2.62% in their next report [14]. After overcoming the problem of residual gases in the sulfurization chamber, the efficiency number rose to 5.45% [44].

This group has also contributed towards sputtered CZTS films followed by sulfurization [43] and reported an efficiency of 6.7%. They observed that soaking the CZTS layer on the Mo coated sodalime glass in deionized water leads to significant improvement in the device performance. Recently, they also reported 6.48% efficiency using CZTS compound target and a simple single sputtering step [45].

In 2010, IBM group reported an efficiency of 6.8% by using co-evaporated film of Cu, Zn, Sn and S sources followed by reactive annealing [46]. The best efficiency so far for pure sulfide phase CZTS is 8.4% [39], as noted in the IBM group report for evaporated CZTS films. Also, they recently reported an efficiency for pure selenide phase using co-evaporation is 8.9% [47]. An NREL group reports the best efficiency for pure selenide phase CZTSe as 9.15% [48]. The highest reported efficiency using vacuum based techniques is 9.3% [49], which is for mixed CZTSeS phase using co-sputtering of compound targets followed by annealing at a higher temperature. This report is by an industrial research group ( AQT Solar ).

Some other notable recent reports on vacuum based approaches are as follows:

1. In the quest to obtain Cd-free devices, the researchers at Solar Frontier, Japan recently demonstrated an efficiency of 6.3% for In-based hetero-junction partners and 5.8% for Zn-based hetero-junction partners [50].
2. The same group in Japan reports > 8% efficiency on CZTS sub-module [51]. Another interesting and note-worthy contribution here is that the absorber thickness is reported to be just 600 nm.
3. Salomé et al demonstrate that incorporation of H<sub>2</sub> is beneficial for preventing Zn loss during the sulfurization [52].
4. Shin et al mention that stacking of precursors has a role in getting single-phase final CZTS compound and reducing the secondary phases [53].
5. Chalapathy and co-workers demonstrate an efficiency of 4.59% using ZnSn (60:40at%) alloy target [54].

### 2.5.2. Electrodeposition

Electro-deposition is of particular interest for the thin film photovoltaics community due to the advantages it offers: low cost, environment friendly, large area deposition, room temperature growth, and less or almost no wastage of materials. CIGS technology based on electro-deposition has already been commercialized [55]. There are numerous reports on electro-deposition of CZTS as well [29,56,57]. Most of the reported efficiencies are in the range of 3% to 4% for electro-deposited CZTS films [57-59].

Some other notable recent reports on electro-deposited CZTS films are as follows:

1. Li et al recently demonstrated 1.7% efficiency in CZTSe films prepared by co-electro-deposition [60].
2. Mali et al used a successive ionic layer adsorption and reaction (SILAR) method for CZTS films. In this method, a substrate is immersed into separately placed cations and anions. This particular electro-chemical method is used for making uniform and large area thin films [61].

### 2.5.3. *Spray pyrolysis*

Spray pyrolysis is a versatile as well as a low-cost technique that has been used to deposit semiconductor films. In this process, a thin film is deposited by spraying a solution on a hot surface. The constituents react to form a chemical compound. The chemical reactants are selected such that the products other than the desired compound are volatile at the temperature of deposition [62]. There have been early reports of sprayed CZTS films [33].

Some other notable recent reports on sprayed CZTS films are as follows:

1. Prabhakar et al prepared CZTS films using ultrasonic spray pyrolysis and observed that sodium plays an important role in CZTS films as well [63]. This observation similar to CIGS films and the role of sodium in CIGS films is well known. The authors observed that sodium enhanced (112) orientation and grain size of the CZTS films also increased the hole carrier concentration.
2. In another report, authors prepared CZTS films using two different tin precursors: stannous as well as stannic chloride [64]. They observed that crystallinity and grain size as well as carrier concentration and mobility values were better for films prepared using stannic chloride.

### 2.5.4. *Solution based methods*

Direct liquid deposition or 'ink' based approaches are attractive due to their compatibility with high volume manufacturing techniques such as printing. It is a low-cost scalable route for the thin film solar technology. One of the popular approaches is to prepare precursors using sol-gel method, then sulfurize it, and deposit on substrate using spin-coating [65]. The micro-particles of CZTS have also been prepared using ball milling, sintering type of processes and later screen printed on flexible substrates [66]. There are various other reports using colloidal nanoparticles [67], Photochemical deposition [30] etc.

The researchers at IBM in their recent publication have reported the highest record efficiency by any process so far for CZTSeS as 10.1% [38]. The J-V curve of this record sample and cross-section of the CZTSeS film is as shown in Fig. 4. Here metal chalcogenides were dissolved in hydrazine solution and later spin-coated on glass-substrates followed by a heat-treatment at 540°C.

Some other notable recent reports on solution/ink based CZTS films are as follows:

1. Using band-gap engineering with Germanium, researchers at Purdue University have achieved an efficiency of 8.4%. They have utilized nanoparticles of CZTSeS on Moly-coated glass substrates [68].
2. The researchers at DuPont have demonstrated an efficiency of 8.5% [69]. They use binary and ternary chalcogenide nanocrystals produced by simple colloidal syntheses.

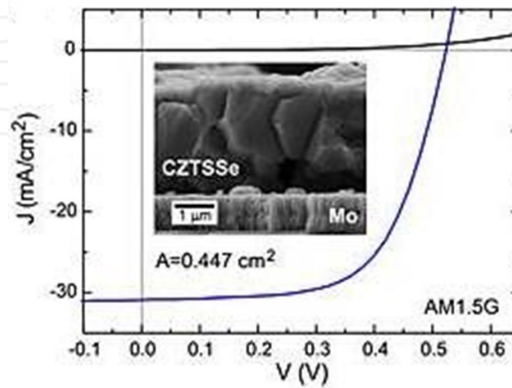


**Figure 4.** J–V characteristics of the record 10.1% sample at AM1.5G simulated illumination along-with CZTSSe film cross-section (Reprinted from [38] with permission from John Wiley and Sons).

## 2.6. Current status

The laboratory level efficiencies are more than 10% [38] and there are some recent reports of sub-module efficiencies of more than 8% [51]. However, the technology still needs to go a long way before it can be commercialized. The complex phase diagram and material properties impose most of the challenges. Also, the narrow stoichiometry window for a stable CZTS phase requires a robust control on composition. The processing window is even narrower compared to their CIGS counterparts. The volatile nature of some components, such as tin sulfide and zinc, impedes further challenges for traditional vacuum-based processing approaches which require high sulfurization/selenization temperatures after precursor deposition. The secondary phases formed are difficult to detect with conventional techniques such as XRD due to the overlapping peaks with pure CZTS phase. The interface properties with hetero-junction partners need to be studied well. However, the initial results in last few years look quite promising.

## 3. Zinc phosphide ( $Zn_3P_2$ )

### 3.1. Introduction

With rise in the prices and non-abundance of the materials such as indium and gallium current research trends in thin film solar cells have been moving toward development of earth-abundant solar cell materials that can be synthesized using low-cost processes. Also, zinc-based hetero-junction partners are preferred over toxic cadmium based compounds such as Cadmium sulfide [70]. Zinc phosphide ( $Zn_3P_2$ ) is an important optoelectronic material,

which also has applications in lithium ion batteries [71]. It is an important semiconductor from the II-V group, and is used for optoelectronic applications [13,72-74]. Zinc phosphide exhibits favorable optoelectronic properties, such as direct bandgap of 1.5 eV, which corresponds to the optimum solar energy conversion range [74-77]. Zinc phosphide has a large optical absorption coefficient of  $>10^4 \text{ cm}^{-1}$ , hence it can be positively used as a p-type absorber [78]. Also, due to its long minority diffusion length of  $\sim 10 \mu\text{m}$ , high current collection efficiency can be yielded. Zinc, as well as phosphorous, is abundant in the earth's crust. This makes their cost-effective development quite feasible when it comes to large scale production [73,79]. Zinc phosphide is a tetragonal p-type low cost material with lattice constants of  $a = b = 8.097 \text{ \AA}$  and  $c = 11.45 \text{ \AA}$  [17] and has all the right characteristics for photo conversion.  $\text{Zn}_3\text{P}_2$  is synthesized most of times with a p-type conductivity [80].

### 3.2. Early efforts

Thin film solar cell devices using  $\text{Zn}_3\text{P}_2$  have been fabricated using Schottky contacts, p-n semiconductor hetero-junctions [81] or liquid contacts [82]. Zinc phosphide was explored extensively in the early eighties and nineties [11,78,80,83,84]. With a Schottky diode, an efficiency as high as 6% was demonstrated [78]. Zinc phosphide homo-junctions have been difficult to make. However, even a zinc phosphide hetero-junction solar cell has not been successful with an efficiency range around 2% [11,85,86].

The researchers at the Institute of Energy Conversion were leaders in the early eighties in exploring  $\text{Zn}_3\text{P}_2$  [78,80,83,87,88]. They demonstrated the effect of Mg doping and also fabricated Schottky barrier solar cells [78,88]. They also successfully made hetero-junction solar cells using ZnO as a hetero-junction partner [11].

Another interesting study is by Misiewicz et al [89]. They made various metal contacts (Au, Ag, Sb, Al, Mg) with  $\text{Zn}_3\text{P}_2$  and measured current-voltage characteristics. It was observed that Ag and Sb made the best ohmic contacts, while Au, Mg and Al exhibited rectifying properties. Mg was found to be the most useful for making Schottky barriers.

### 3.3. Synthesis techniques

Some of the synthesis techniques to grow  $\text{Zn}_3\text{P}_2$  are summarized below :

#### 3.3.1. Vapor transport

Catalano et al [90] report synthesis of  $\text{Zn}_3\text{P}_2$  by vapor transport using perforated capsule technique. Crystals were grown in silica tubes placed mid-way in a capsule immediately ahead of  $\text{Zn}_3\text{P}_2$  charge. When heated at a high temperature ( $900^\circ\text{C}$ ), effusion of zinc and phosphorous out of the inner growth capsule resulted in the condensation of  $\text{Zn}_3\text{P}_2$  on the walls of outer tube's cooler portion. A similar vapor transport technique has been reported by Wang et al [91] for growing single crystal  $\text{Zn}_3\text{P}_2$ .

#### 3.3.2. Evaporation

Deiss et al report synthesis of  $\text{Zn}_3\text{P}_2$  thin film by direct evaporation of  $\text{Zn}_3\text{P}_2$  on glass substrates in a vacuum chamber at  $750^\circ\text{C}$  [92]. The films deposited on a cold substrate were re-

ported as amorphous, while the films deposited on a heated substrate ( $>300^{\circ}\text{C}$ ) were reported as crystalline. In a similar technique, Murali et al report that films grown with source-substrate distance  $< 3$  cm were crystalline in nature [93].

### 3.3.3. Metal organic chemical vapor deposition (MOCVD)

Kakishita et al report a low-pressure MOCVD system with dimethylzinc (DMZ) and diluted phosphine ( $\text{PH}_3$ ) as reactant gas [72]. Phosphine was cracked at  $800^{\circ}\text{C}$  and  $\text{Zn}_3\text{P}_2$  films were grown on ZnSe single crystal substrates at a growth temperature of  $290\text{--}410^{\circ}\text{C}$ . Hermann et al report use of diethylzinc (DEZ) as a zinc precursor [15].

### 3.3.4. Electrodeposition

Soliman et al [94] report electrodeposition of  $\text{Zn}_3\text{P}_2$  with  $\text{SnO}_2$  coated glass as working electrode and the aqueous solution containing different concentrations of both  $\text{ZnCl}_2$ ,  $\text{ZnSO}_4$  and  $\text{Na}_2\text{PO}_3$ . The pH was adjusted at 2.5 by adding  $\text{H}_2\text{SO}_4$ . It was observed that  $\text{Zn}_3\text{P}_2$  was obtained, and the degree of crystallinity increased with higher Zn/P molar ratio. There is a recent report similar to that of Soliman et al, reporting electrodeposition of  $\text{Zn}_3\text{P}_2$  [95].

### 3.3.5. Chemical reflux technique

Recently our group has successfully synthesized  $\text{Zn}_3\text{P}_2$  using chemical reflux technique [96,97]. The zinc-coated glass substrate is placed on the top of a fritted glass, which is surrounded by trioctylphosphine (TOP) liquid. The entire vessel is heated while vapors of TOP are refluxed back to the bottom of the glass vessel by a condenser connected at the top of the vessel. The glass vessel is heated to  $350^{\circ}\text{C}$  for two to four hours, and then slowly cooled to room temperature. It was observed that zinc phosphide can be successfully synthesized using this simple chemical route in both nano-wire and thin film forms depending on the exposure mechanism of the phosphorous precursor with the zinc-deposited substrates.

## 3.4. Current status

Recently Kimball et al have studied the effect of magnesium doping on  $\text{Zn}_3\text{P}_2$  thin films [98,99]. Our group has recently demonstrated that zinc phosphide can be successfully synthesized in both nano-wire and thin film forms [96,97]. Efforts are ongoing to improve the photovoltaic properties using various hetero-junction partner options.

## 4. Iron disulfide ( $\text{FeS}_2$ )

### 4.1. Introduction

Pyrite ( $\text{FeS}_2$ ) is a non-toxic material and is abundant on earth, and has a potential to be an inexpensive and sustainable alternative for achieving low-cost and high-efficiency solar cells due both to its environmental compatibility and its optimal optical properties for efficient energy conversion. Its energy band gap of 0.95 eV and optical absorption coefficient of the

order of  $10^5 \text{ cm}^{-1}$  are in the optimal range for efficient conversion of sunlight into electricity [12,100]. A saturation current of 40 to 50 mA/cm<sup>2</sup> for a thickness between 0.2  $\mu\text{m}$  to 1  $\mu\text{m}$  is possible for pyrite [101]. In addition, a carrier mobility of 200 cm<sup>2</sup>/Vs and sufficiently high minority carrier lifetimes makes pyrite highly favorable for photovoltaic application [102]. It has been calculated that theoretical conversion efficiency close to 30% is possible because its band gap is quite close to silicon.

Iron pyrite, like other metal chalcogenides, received considerable attention after the photo-electrochemical solar cells using FeS<sub>2</sub> single crystal electrodes in contact with iodide/tri-iodide (I<sup>-</sup>/I<sub>3</sub><sup>-</sup>) redox electrolyte exhibited a quantum efficiency close to 100% across a n-FeS<sub>2</sub>/(I<sup>-</sup>/I<sub>3</sub><sup>-</sup>) interface [103-105]. However, a solar conversion efficiency of this photochemical cell was only 2.8% when illuminated under AM 1.5. The open circuit voltage ( $V_{oc}$ ) was 187 mV. This value of  $V_{oc}$  is lower than the theoretical value of about 500 mV [106]. The low photopotential is attributed to the strong pinning of the Fermi level caused by surface states [105] as well as bulk defects caused by the sulphur deficiency [107].

It should be noted that numerous iron sulphides exist in nature with unique properties depending on different iron (Fe) and sulphur (S) stoichiometric ratios and different crystal structures. Thus creating a phase pure iron pyrite is a challenge. Orthorhombic marcasite FeS<sub>2</sub> and hexagonal troilite FeS are both common iron sulfur phases, but because they have much smaller band gaps (0.34 eV for marcasite and 0.04 eV for troilite), even trace amounts would significantly diminish the photovoltaic properties of the pyrite [108]. So, examining the preparation of pyrite by using various techniques is important.

## 4.2. Synthesis techniques

Some of the experimental techniques used to grow pyrite are summarized below:

### 4.2.1. Chemical vapor transport (CVT)

This technique involves high crystal growth with halogens, such as Br<sub>2</sub> and Cl<sub>2</sub>, and polycrystalline FeS<sub>2</sub> sealed in an ampoule [109]. This process produced cubic crystals with (111) and (100) faces up to 5 mm edge length. However, the growth process was too long (10 days) and was performed at high temperature (~1000°C). At elevated temperatures, segregation of sulphur and iron species is unavoidable.

### 4.2.2. Metal organic chemical vapor deposition (MOCVD)

Iron source, such as iron penta-carbonyl [Fe (CO)<sub>5</sub>], and sulphur sources such as sulphur and H<sub>2</sub>S gas, are used in this technique [102]. The advantage of this technique is that the growth temperature is low (150°C) and the growth process is fast.

### 4.2.3. Spray pyrolysis

Chemical spray pyrolysis is used to grow FeS<sub>2</sub> using thiourea and FeCl<sub>2</sub> [110]. Chlorine contamination, slow growth, non-uniformity, reduced repeatability are some issues associated with this technique.

#### 4.2.4. Chemical methods

A recent synthesis approach to grow a single phase FeS<sub>2</sub> nanoparticle is carried out by different groups using hydrothermal process [108,111]. Wadia and his group show single phase growth of FeS<sub>2</sub> nanoparticles. On the other hand, colloidal FeS<sub>2</sub> nano-crystal ink by using a hot-injection method has been synthesized by many groups [112-116]. These processes are encouraging in that these are low temperature processes and variation in particle sizes allows the manipulation of band gap, which will help to absorb a broader spectrum of sunlight. To translate these nanocrystals into a form of a compact thin film layer is a challenge [113,116,117].

#### 4.2.5. Sulfurization of iron oxides

Sulphurization of iron oxides (Fe<sub>3</sub>O<sub>4</sub> or Fe<sub>2</sub>O<sub>3</sub>) is predicted by Gibbs free energy phase diagram to give FeS<sub>2</sub> films [118]. Smestad et. al, sulphurized Fe<sub>3</sub>O<sub>4</sub> or Fe<sub>2</sub>O<sub>3</sub> using gaseous sulphur at 350°C. However, they didn't observe a good photovoltaic behavior from the photochemical cells made by using the FeS<sub>2</sub> films grown this way. One of the main reasons attributed to the poor photocurrent and voltage is the presence of micro-pinholes, which led to a short circuit in the photogenerated current and effectively shunted the pyrite cell. Recently, defect-free pyrite thin films were synthesized from iron oxide by using non-toxic and a more controllable organic precursor such as Di-tert butyl disulfide (TBDS) [119].

#### 4.2.6. Sulfurization of iron

It is also claimed by another group that iron oxide route is not necessary to grow pyrite [12]. They used iron film and sulphurized it under nitrogen flux. But their films had a presence of an amorphous phase, which caused an indirect transition at 1.31 eV incompatible with the strong absorption of FeS<sub>2</sub>

### 4.3. Issues to be addressed for an optimal FeS<sub>2</sub> cell

Low open circuit ( $V_{oc}$ ) in pyrite solar cell is attributed to sulphur deficiency among other reasons [120]. A correlation between S deficiency and the transport parameters of pyrite was found, indicating that high quality intrinsic material can be prepared when the S/Fe ratio is close to the stoichiometric value of 2 [121]. In addition to the intrinsic material property, a device design would also affect  $V_{oc}$ .

#### 4.3.1. Influence of cell design on $V_{oc}$

The electrical and optical properties of FeS<sub>2</sub> are promising for an efficient photovoltaic action, but the conversion efficiency of the FeS<sub>2</sub> cell is not impressive: 1% with Schottky type solar cells [101] and 2.8% with photochemical cells. Cells fabricated with Schottky contacts exhibited short circuit currents ( $J_{sc}$ ) below 10 mA/cm<sup>2</sup> and open circuit voltages ( $V_{oc}$ ) below 20 mV. However, quantum efficiencies of 90% and above and high photo-current density observed in the latter type of the cell indicate the potential of an efficient pyrite based solar cell. The reason for the low efficiency was due to low open circuit volt-

age of about 200 mV. The interfacial chemistry of the p-n junction plays a role in dictating the open circuit voltage. A solar cell structure with a wide band gap window layer, such as ZnS, may improve the open circuit voltage.

#### 4.3.2. Stoichiometry of $\text{FeS}_2$

The ratio of Fe and S is extremely important to obtain a defect-free  $\text{FeS}_2$  phase. It is necessary that the homogeneity range should be within 1%. It was shown in pyrite grown by MOCVD that whenever a stoichiometry is such that the composition of S is less than 2, a phase mixture of pyrite and pyrrhotite ( $\text{FeS}$ ) existed. The band gap of pyrrhotite phase is 0.04 eV, which greatly diminishes the photovoltaic action. Thus reaffirmation of the pyrite stoichiometry is important.

#### 4.3.3. Influence of doping on $V_{oc}$

A recent work on simulation of p-n type  $\text{FeS}_2$  homo-junction diffusion limited solar cells showed that efficiencies around 20% are possible [101] by assuming that at low doping density Shockley–Read–Hall (SRH) recombination [122,123] limits the carrier life time, or in other words, the cell efficiency. Altermatt et. al [101] simulated a case where the carrier life time ( $t$ ) limits only  $V_{oc}$  e.g. a cell with  $d = 1 \mu\text{m}$  and  $t = 100 \text{ ns}$ . The optimally obtainable photocurrent in pyrite under AM 1.5G illumination is about  $50 \text{ mA/cm}^2$ . The achievable efficiency level then was 18.5% (13.5%) in a highly (lowly) doped cell. There is trade-off between the carrier life time and open circuit voltage. For a high density of carriers, the voltage across the junction increases, which may create a higher  $V_{oc}$  provided the recombination of the generated carriers is prevented. This is possible with the low carrier density (thus low dopant induced defects) case where the carrier life time is longer. Thus a subtle balance between  $V_{oc}$  and excess carrier life time should be sought by carefully choosing the right dopant density. It was observed in Cobalt doped  $\text{FeS}_2$  that by manipulating the carrier concentration, the grain barrier height can be changed, which in turn will change the photo-voltage [124].

#### 4.3.4. Fermi level pinning at the surface

Low photo-voltage in a pyrite solar cell is dependent upon its surface structure. Ultraviolet photoemission spectroscopy (UPS) measurements carried out in Cobalt doped  $\text{FeS}_2$  showed that the Fermi level at the surface is pinned [125], implying high density of surface. Thus controlling the dopant density with a high level of precision is critical. In a situation where surface defects are unavoidable, application of a resistive thin layer, such as n-type i-ZnO, could be helpful.

### 4.4. Recent progress in $\text{FeS}_2$ solar cell device

Recently Ganta et. al fabricated solid state based  $\text{FeS}_2$  thin film solar cell using CdS as an n-type layer [116]. The super-strate type cell structure was glass/FTO/CdS/ $\text{FeS}_2$ /Ag/Cr.  $\text{FeS}_2$  layer was formed by drop casting the  $\text{FeS}_2$  nanoparticle ink directly onto the CdS layer at room temperature. The efficiency for CdS/ $\text{FeS}_2$  cell was 0.03%. The low efficiency was due to

the low short-circuit current. The open-circuit voltage was high, which is large compared to a previously reported value of 200 mV [106].

Although the circuit current was low at  $0.01 \text{ mA/cm}^2$ , an open-circuit voltage of 565 mV was observed. Residual organic components present in the nanoparticle-film could be a reason for low short-circuit current. A compact film with the organic residues removed can be expected to improve the short-circuit current and the cell efficiency.

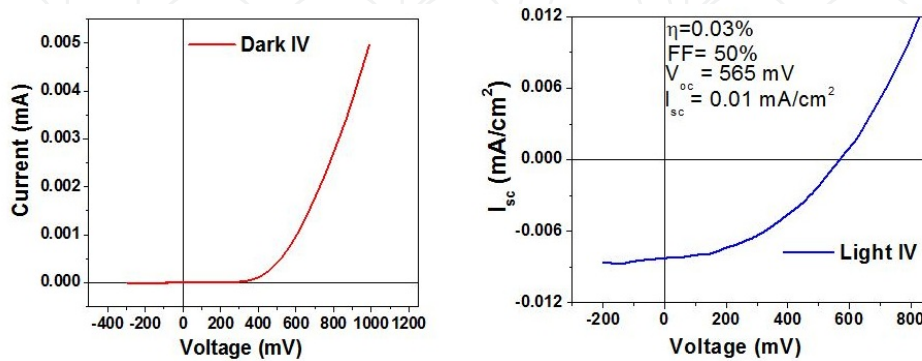


**Figure 5.** Dark and light I-V curves of the  $\text{FeS}_2$  super-strate solar cell.

## 5. Other earth-abundant candidates

In a recent study, a number of materials were screened based on their abundance and non-toxicity, and semiconducting compounds composed of these identified materials were listed [126]. The authors found that even if binary compounds are focused, there are a good number of alternatives. Once semiconducting properties such as ideal band-gap and minority carrier diffusion length are considered, the next step is the processing capability. Obtaining the right phase without any defects is crucial. The next step is to identify ideal hetero-junction partner with right band-alignment as well as chemical and mechanical compatibility. Several other earth-abundant candidates are being researched these days.

Tin Sulfide ( $\text{SnS}$ ) is metal chalcogenide semiconductor material from the IV-VI group. It has a near optimum direct bandgap of  $\sim 1.3 \text{ eV}$  [127] and also a good absorption co-efficient ( $10^5 \text{ cm}^{-1}$ ) [128]. Elements such as tin and sulfur are abundantly available. Tin sulfide has been synthesized using a variety of techniques such as sputtering [127], evaporation [129], electrodeposition [130] as well as chemical routes [131]. The highest reported efficiency to date is 1.3% [132].

$\text{Cu}_2\text{FeSnS}_4$  (CFTS) with Stannite structure can also be a viable alternative and there are some recent reports of growing CFTS nanocrystals [133,134]. The bandgap of CFTS was found to be  $\sim 1.28 \text{ eV}$  with p-type conductivity [134].

In a recent study, Fernandes et al identified ternary sulfides  $\text{Cu}_2\text{SnS}_3$  and  $\text{Cu}_3\text{SnS}_4$  as good alternatives [135]. The estimated bandgap values are between 1 to 1.6 eV and absorption coefficient  $10^4 \text{ cm}^{-1}$ .

Cu<sub>2</sub>S is another interesting material that was extensively researched in the eighties. However, performance degradation due to copper diffusion led this technology to be abandoned. Cu<sub>2</sub>S has a bandgap of 1.2 eV [136]. The highest reported efficiency was 9.1% [137]. Recently this material has again received attention and innovative approaches, such as nanocrystals, are being implemented to overcome the issues encountered in the past [138].

## 6. Conclusion

One of the important p-type absorber CZTSe(S) has reached a laboratory level efficiency of more than 10% and has matured to a stage where it can be seriously considered for commercialization. Complex phase diagram and narrow stoichiometry window for CZTS remains a challenge; in addition, interface properties with suitable hetero-junction partners need to be understood better. However, despite these challenges, CZTS is the most promising material synthesized using earth-abundant constituents. Other materials discussed in detail in this review are Zn<sub>3</sub>P<sub>2</sub> and FeS<sub>2</sub>. These two materials also show considerable promise, despite their current low lab-level efficiency values. Apart from these, there are several other promising materials synthesized using earth-abundant constituents, such as SnS, CFTS and Cu<sub>2</sub>SnS<sub>3</sub>, and these potentially can be used in solar cells due to their photovoltaic properties.

## Author details

Parag S. Vasekar\* and Tara P. Dhakal

\*Address all correspondence to: [psvasekar@yahoo.com](mailto:psvasekar@yahoo.com), [tpdhakal@gmail.com](mailto:tpdhakal@gmail.com)

Center for Autonomous Solar Power, Binghamton University, Binghamton, NY, USA

## References

- [1] Loferski, J. J. J. (1956). Theoretical Considerations Governing the Choice of the Optimum Semiconductor for Photovoltaic Solar Energy Conversion. *J Appl Phys*, 27, 777.
- [2] Shockley, W.W. (1961). Detailed Balance Limit of Efficiency of p-n Junction Solar Cells. *J Appl Phys*, 32, 510.
- [3] Green, M. A., Emery, K., Hishikawa, Y., Warta, W., & Dunlop, E. D. (2011). Solar cell efficiency tables (Version 38). *Prog Photovoltaics Res Appl*, 19, 565-72.
- [4] Guha, S.S. (1986). Enhancement of open circuit voltage in high efficiency amorphous silicon alloy solar cells. *Appl Phys Lett*, 49, 218.

- [5] Gordon, I., Carnel, L., Van Gestel, D., Beaucarne, G., & Poortmans, J. (2007). Efficient thin-film polycrystalline-silicon solar cells based on aluminum- induced crystallization and thermal CVD. *Prog Photovoltaics Res Appl*, 15, 575-86.
- [6] Jackson, P., Hariskos, D., Lotter, E., Paetel, S., Wuerz, R., Menner, R., et al. (2011). New world record efficiency for Cu(In,Ga)Se<sub>2</sub> thin-film solar cells beyond 20%. *Prog Photovoltaics Res Appl*, 19, 894-7.
- [7] Wu, X. X. (2004). High-efficiency polycrystalline CdTe thin-film solar cells. *Solar Energy*, 77, 803-14.
- [8] Katagiri, H., Jimbo, K., Maw, W. S., Oishi, K., Yamazaki, M., Araki, H., et al. (2009). Development of CZTS-based thin film solar cells. *Thin Solid Films*, 517, 2455-60.
- [9] Wadia, C. C. (2009). Materials Availability Expands the Opportunity for Large-Scale Photovoltaics Deployment. *Environ Sci Technol*, 43, 2072-7.
- [10] Liu, F., Li, Y., Zhang, K., Wang, B., Yan, C., Lai, Y., et al. (2010). In situ growth of Cu<sub>2</sub>ZnSnS<sub>4</sub> thin films by reactive magnetron co-sputtering. *Solar Energy Mater Solar Cells*, 94, 2431-4.
- [11] Nayar, P. P. S. (1981). Zinc phosphide-zinc oxide heterojunction solar cells. *Appl Phys Lett*, 39, 105.
- [12] Rezig, B., Dahman, H., & Kenzari, M. (1992). Iron pyrite FeS<sub>2</sub> for flexible solar cells. *Renewable Energy*, 2, 125-8.
- [13] Babu, V. S., Vaya, P. R., & Sobhanadri, J. (1988). Optical absorption and photoconductivity studies on Zn<sub>3</sub>P<sub>2</sub> thin films grown by hot wall deposition. *Solar Energy Materials*, 18, 65-73.
- [14] Katagiri, H. H. (2001). Development of thin film solar cell based on Cu<sub>2</sub>ZnSnS<sub>4</sub> thin films. *Solar Energy Mater Solar Cells*, 65, 141-8.
- [15] Hermann, A. M., Madan, A., Wanlass, M. W., Badri, V., Ahrenkiel, R., Morrison, S., et al. (2004). MOCVD growth and properties of Zn<sub>3</sub> P<sub>2</sub> and Cd<sub>3</sub>P<sub>2</sub> films for thermal photovoltaic applications. *Solar Energy Mater Solar Cells*, 82, 241-52.
- [16] Morsli, M. M. (1995). Electrical Properties of a Synthetic Pyrite FeS Non Stoichiometric Crystal. *Journal de physique.I : JP*, 5, 699-705.
- [17] Sudhakar, S.S. (2008). Influence of cooling rate on the liquid-phase epitaxial growth of Zn<sub>3</sub> P<sub>2</sub>. *J Cryst Growth*, 310, 2707-11.
- [18] Dhere, N. G. (2007). Toward GW/year of CIGS production within the next decade. *Solar Energy Materials and Solar Cells*, 91, 1376-82.
- [19] Dhere, N. G. (2011). Scale-up issues of CIGS thin film PV modules. *Solar Energy Mater Solar Cells*, 95, 277-80.
- [20] Green, M. M. A. (2006). Consolidation of thin-film photovoltaic technology: the coming decade of opportunity. *Progress in photovoltaics*, 14, 383-92.

- [21] Anderson, B. A., Azar, C., Holmberg, J., & Karlsson, S. (1998). Material constraints for thin-film solar cells. *Energy*, 23, 407-11.
- [22] Katagiri, H. (2005).  $\text{Cu}_2\text{ZnSnS}_4$  thin film solar cells. *Thin Solid Films*, 480, 426.
- [23] Fischereder, A. A. (2010). Investigation of Cu ZnSnS Formation from Metal Salts and Thioacetamide. *Chemistry of materials*, 22, 3399-406.
- [24] Katagiri, H., Sasaguchi, N., Hando, S., Hoshino, S., Ohashi, J., & Yokota, T. (1997). Preparation and evaluation of  $\text{Cu}_2\text{ZnSnS}_4$  thin films by sulfurization of E---B evaporated precursors. *Solar Energy Mater Solar Cells*, 49, 407-14.
- [25] Araki, H. (2008). Preparation of  $\text{Cu}_2\text{ZnSnS}_4$  thin films by sulfurization of stacked metallic layers. *Thin Solid Films*, 517, 1457.
- [26] Seol, J., Lee, S., Lee, J., Nam, H., & Kim, K. (2003). Electrical and optical properties of  $\text{Cu}_2\text{ZnSnS}_4$  thin films prepared by rf magnetron sputtering process. *Solar Energy Mater Solar Cells*, 75, 155-62.
- [27] Tanaka, T., Kawasaki, D., Nishio, M., Guo, Q., & Ogawa, H. (2006). Fabrication of  $\text{Cu}_2\text{ZnSnS}_4$  thin films by co-evaporation. *physica status solidi (c)*, 3, 2844-7.
- [28] Tanaka, T., Nagatomo, T., Kawasaki, D., Nishio, M., Guo, Q., Wakahara, A., et al. (2005). Preparation of  $\text{Cu}_2\text{ZnSnS}_4$  thin films by hybrid sputtering. *Journal of Physics and Chemistry of Solids*, 66, 1978-81.
- [29] Araki, H., Kubo, Y., Mikaduki, A., Jimbo, K., Maw, W. S., Katagiri, H., et al. (2009). Preparation of  $\text{Cu}_2\text{ZnSnS}_4$  thin films by sulfurizing electroplated precursors. *Solar Energy Mater Solar Cells*, 93, 996-9.
- [30] Moriya, K., Watabe, J., Tanaka, K., & Uchiki, H. (2006). Characterization of  $\text{Cu}_2\text{ZnSnS}_4$  thin films prepared by photo-chemical deposition. *physica status solidi (c)*, 3, 2848-52.
- [31] Tanaka, K., Oonuki, M., Moritake, N., & Uchiki, H. (2009).  $\text{Cu}_2\text{ZnSnS}_4$  thin film solar cells prepared by non-vacuum processing. *Solar Energy Mater Solar Cells*, 93, 583-7.
- [32] Yeh, M. M. Y. (2009). Influences of synthesizing temperatures on the properties of  $\text{Cu}_2\text{ZnSnS}_4$  prepared by sol-gel spin-coated deposition. *J Sol Gel Sci Technol*, 52, 65-8.
- [33] Nakayama, N., & Ito, K. (1996). Sprayed films of stannite  $\text{Cu}_2\text{ZnSnS}_4$ . *Appl Surf Sci*, 92, 171-5.
- [34] Kamoun, N., Bouzouita, H., & Rezig, B. (2007). Fabrication and characterization of  $\text{Cu}_2\text{ZnSnS}_4$  thin films deposited by spray pyrolysis technique. *Thin Solid Films*, 515, 5949-52.
- [35] Riha, S. C., Parkinson, B. A., & Prieto, A. L. (2009). Solution-Based Synthesis and Characterization of  $\text{Cu}_2\text{ZnSnS}_4$  Nanocrystals. *J Am Chem Soc*, 131, 12054-5.
- [36] Todorov, T. K., Reuter, K. B., & Mitzi, D. B. (2010). High-Efficiency Solar Cell with Earth-Abundant Liquid-Processed Absorber. *Adv Mater*, 22, E 156-9.

- [37] K. Ito, T.N. (1988). Electrical and optical properties of stannite-type quaternary semiconductor thin films. *Japanese journal of Applied Physics*.
- [38] Barkhouse, D. A. R., Gunawan, O., Gokmen, T., Todorov, T., & Mitzi, D. (2012). Device characteristics of a 10.1% hydrazine-processed  $\text{Cu}_2\text{ZnSn}(\text{Se,S})_4$  solar cell Characteristics of a 10.1% efficient kesterite solar cell. *Progress in photovoltaics*, 20, 6-11.
- [39] Shin, B., Gunawan, O., Zhu, Y., Bojarczuk, N. A., Chey, S. J., & Guha, S. (2011). Thin film solar cell with 8.4% power conversion efficiency using an earth-abundant  $\text{Cu}_2\text{ZnSnS}_4$  absorber. *Prog Photovoltaics Res Appl:n/a,n/a*.
- [40] Stanbery, B. B. J. (2002). Copper Indium Selenides and Related Materials for Photovoltaic Devices. *Critical reviews in solid state and materials sciences*, 27, 73-117.
- [41] Siebentritt, S. S. (2012). Kesterites-a challenging material for solar cells Kesterites-a challenging material for solar cells. *Progress in photovoltaics:n,a-n/a*.
- [42] Olekseyuk, I. D. (2004). Phase equilibria in the  $\text{Cu}_2\text{S-ZnS-SnS}_2$  system. *J Alloys Compounds*, 368, 135-43.
- [43] Katagiri, H. (2008). Enhanced conversion efficiencies of  $\text{Cu}_2\text{ZnSnSP4}$  based thin film solar cells by using preferential etching technique. *Applied physics express*, 1.
- [44] Katagiri, H., Jimbo, K., Moriya, K., & Tsuchida, K. (2003). Solar cell without environmental pollution by using CZTS thin film. *Photovoltaic Energy Conversion, Proceedings of 3rd World Conference on*, 3, 2874-2879.
- [45] Katagiri, H., & Jimbo, K. (2011). Development of rare metal-free CZTS-based thin film solar cells. *Photovoltaic Specialists Conference (PVSC), 37th IEEE*, 003516-21.
- [46] Wang, K., Gunawan, O., Todorov, T., Shin, B., Chey, S. J., Bojarczuk, N. A., et al. (2010). Thermally evaporated  $\text{Cu}_2\text{ZnSnS}_4$  solar cells. *Appl Phys Lett*, 97, 143508.
- [47] Shin, B., Zhu, Y., Bojarczuk, N. A., Chey, S. J., & Guha, S. (2012). High efficiency  $\text{Cu}_2\text{ZnSnSe}_4$  solar cells with a TiN diffusion barrier on the molybdenum bottom contact. *38th IEEE Photovoltaic Specialists Conference (PVSC)*.
- [48] Repins, I., Beall, C., Vora, N., De Hart, C., Kuciauskas, D., Dippo, P., et al. (2012). Co-evaporated  $\text{Cu}_2\text{ZnSnSe}_4$  films and devices. *Solar Energy Mater Solar Cells*, 101, 154-9.
- [49] Chawla, V., & Clemens, B. (2012). Effect of Composition on High Efficiency CZTS<sub>Se</sub> Devices Fabricated Using Co-sputtering of Compound Targets. *38th IEEE Photovoltaic Specialists Conference (PVSC)*.
- [50] Hiroi, H., Sakai, N., Muraoka, S., Katou, T., & Sugimoto, H. (2012). Development of High Efficiency  $\text{Cu}_2\text{ZnSnS}_4$  Submodule with Cd-Free Buffer Layer. *38th IEEE Photovoltaic Specialists Conference (PVSC)*.
- [51] Sugimoto, H., Hiroi, H., Sakai, N., Muraoka, S., & Katou, T. (2012). Over 8% Efficiency  $\text{Cu}_2\text{ZnSnS}_4$  Submodules with Ultra-Thin Absorber. *38th IEEE Photovoltaic Specialists Conference (PVSC)*.

- [52] Salomé, P. M. P., Malaquias, J., Fernandes, P., Ferreira, M., Leitao, J., Cunha, A., et al. (2011). The influence of hydrogen in the incorporation of Zn during the growth of  $\text{Cu}_2\text{ZnSnS}_4$  thin films. *Solar Energy Mater Solar Cells*, 95(12), 3482-9.
- [53] Shin, S. W., Pawar, S., Park, C., Yun, J., Moon, J., Kim, J., et al. (2011). Studies on  $\text{Cu}_2\text{ZnSnS}_4$  (CZTS) absorber layer using different stacking orders in precursor thin films. *Solar Energy Mater Solar Cells*, 95(12), 3202-6.
- [54] Chalapathy, R. B. V., Jung, G. S., & Ahn, B. T. (2011). Fabrication of  $\text{Cu}_2\text{ZnSnS}_4$  films by sulfurization of Cu/ZnSn/Cu precursor layers in sulfur atmosphere for solar cells. *Solar Energy Mater Solar Cells*, 95(12), 3216-21.
- [55] Aksu, S., Pethe, S., Kleiman-Shwarsstein, A., Kundu, S., & Pinarbasi, M. (2012). Recent Advances in Electroplating Based CIGS Solar Cell Fabrication. *38th IEEE Photovoltaic Specialists Conference (PVSC)*.
- [56] Scragg, J. J., Dale, P. J., Peter, L. M., Zoppi, G., & Forbes, I. (2008). New routes to sustainable photovoltaics: evaluation of  $\text{Cu}_2\text{ZnSnS}_4$  as an alternative absorber material. *physica status solidi (b)*, 245, 1772-8.
- [57] Scragg, J. J., Berg, D. M., & Dale, P. J. (2010). A 3.2% efficient Kesterite device from electrodeposited stacked elemental layers. *J Electroanal Chem*, 646, 52-9.
- [58] Ennaoui, A. (2009).  $\text{Cu}_2\text{ZnSnS}_4$  thin film solar cells from electroplated precursors: Novel low-cost perspective. *Thin Solid Films*, 517, 2511.
- [59] Araki, H., Kubo, Y., Jimbo, K., Maw, W., Katagiri, H., Yamazaki, M., et al. (2009). Preparation of  $\text{Cu}_2\text{ZnSnS}_4$  thin films by sulfurization of co-electroplated Cu-Zn-Sn precursors. *physica status solidi (c)*, 6, 1266-8.
- [60] Li, J., Wei, T., Liu, M., Jiang, W., & Zhu, G. C. (2012). The  $\text{Cu}_2\text{ZnSnSe}_4$  thin films solar cells synthesized by electrodeposition route. *Appl Surf Sci*, 258, 6261-5.
- [61] Mali, S. S., Shinde, P. S., Betty, C. A., Bhosale, P. N., Oh, Y. W., & Patil, P. S. (2012). Synthesis and characterization of  $\text{Cu}_2\text{ZnSnS}_4$  thin films by SILAR method. *Journal of Physics and Chemistry of Solids*, 73, 735-40.
- [62] Mooney, J. J. B. (1982). Spray Pyrolysis Processing. *Annual review of materials science*, 12, 81-101.
- [63] Prabhakar, T., & Jampana, N. (2011). Effect of sodium diffusion on the structural and electrical properties of  $\text{Cu}_2\text{ZnSnS}_4$  thin films. *Solar Energy Mater Solar Cells*, 95, 1001-4.
- [64] Rajeshmon, V. G., Kartha, C. S., Vijayakumar, K. P., Sanjeeviraja, C., Abe, T., & Kashiwaba, Y. (2011). Role of precursor solution in controlling the opto-electronic properties of spray pyrolysed  $\text{Cu}_2\text{ZnSnS}_4$  thin films. *Solar Energy*, 85, 249-55.
- [65] Tanaka, K., Moritake, N., & Uchiki, H. (2007). Preparation of thin films by sulfurizing sol-gel deposited precursors. *Solar Energy Mater Solar Cells*, 91, 1199-201.

- [66] Zhou, Z., Wang, Y., Xu, D., & Zhang, Y. (2010). Fabrication of  $\text{Cu}_2\text{ZnSnS}_4$  screen printed layers for solar cells. *Solar Energy Mater Solar Cells*, 94, 2042-5.
- [67] Chory, C., Zutz, F., Witt, F., Borchert, H., & Parisi, J. (2010). Synthesis and characterization of  $\text{Cu}_2\text{ZnSnS}_4$ . *physica status solidi (c)*, 7, 1486-8.
- [68] Guo, Q., Ford, G. M., Yang, W., Hages, C. J., Hillhouse, H. W., & Agrawal, R. (2012). Enhancing the performance of CZTSSe solar cells with Ge alloying. *Solar Energy Mater Solar Cells*, 105, 132-6.
- [69] Guo, Q., Cao, Y., Caspar, J., Farneth, W., Ionkin, A., Johnson, L., et al. (2012). A Simple Solution-based Route to High-Efficiency CZTSSe Thin-film Solar Cells. *38th IEEE Photovoltaic Specialists Conference (PVSC)*.
- [70] Kumar, B., Vasekar, P. S., Pethe, S., Dhere, N. G., & Galymzhan, T. (2009).  $\text{Zn}_x\text{Cd}_{1-x}\text{S}$  as a heterojunction partner for  $\text{CuIn}_{1-x}\text{Ga}_x\text{S}_2$  thin film solar cells. *Thin Solid Films*, 517, 2295-9.
- [71] Shen, G., Chen, P., Bando, Y., Golberg, D., & Zhou, C. (2008). Single-Crystalline and Twinned  $\text{Zn}_3\text{P}_2$  Nanowires: Synthesis, Characterization, and Electronic Properties. *The Journal of Physical Chemistry C*, 112, 16405-10.
- [72] Kakishita, K., Aihara, K., & Suda, T. (1994).  $\text{Zn}_3\text{P}_2$  photovoltaic film growth for  $\text{Zn}_3\text{P}_2/\text{ZnSe}$  solar cell. *Solar Energy Mater Solar Cells*, 35, 333-40.
- [73] Misiewicz, J., Bryja, L., Jezierski, K., Szatkowski, J., Mirowska, N., Gumienny, Z., et al. (1994).  $\text{Zn}_3\text{P}_2$  new material for optoelectronic devices. *Microelectron J*, 25, 23-28.
- [74] Lousa, A., Bertrán, E., Varela, M., & Morenza, J. L. (1985). Deposition of  $\text{Zn}_3\text{P}_2$  thin films by coevaporation. *Solar Energy Materials*, 12, 51-6.
- [75] Sathyamoorthy, R., Sharmila, C., Natarajan, K., & Velumani, S. Influence of annealing on structural and optical properties of  $\text{Zn}_3\text{P}_2$  thin films. *Mater Charact*, 58, 745-9.
- [76] Murali, K. R., & Rao, D. R. (1981). Optical band gap of [alpha]-  $\text{Zn}_3\text{P}_2$ . *Thin Solid Films*, 86, 283-6.
- [77] Long, J. (1983). The Growth of  $\text{Zn}_3\text{P}_2$  by Metalorganic Chemical Vapor Deposition. *J Electrochem Soc*, 130, 725-8.
- [78] Bhushan, M. M., & Catalano, A. (1981). Polycrystalline  $\text{Zn}_3\text{P}_2$  Schottky barrier solar cells. *Appl Phys Lett*, 38, 39-41.
- [79] Kakishita, K. (1994). Zinc phosphide epitaxial growth by photo-MOCVD. *Appl Surf Sci*, 79, 281.
- [80] Catalano, A. (1980). Defect dominated conductivity in  $\text{Zn}_3\text{P}_2$ . *The Journal of physics and chemistry of solids*, 41, 635.
- [81] Casey, M. S., Fahrenbruch, A. L., & Bube, R. H. (1987). Properties of zinc-phosphide junctions and interfaces. *Journal of Applied Physics*, 61, 2941-6.

- [82] Bhushan, M., Turner, J. A., & Parkinson, B. A. (1986). Photoelectrochemical Investigation of  $Zn_3P_2$ . *J Electrochem Soc*, 133, 536-9.
- [83] Bhushan, M. M. (1982). Schottky solar cells on thin polycrystalline  $Zn_3P_2$  films. *Appl Phys Lett*, 40, 51.
- [84] Wyeth, N. C., & Catalano, A. (1979). Spectral response measurements of minority-carrier diffusion length in  $Zn_3P_2$ . *Journal of Applied Physics*, 50, 1403-7.
- [85] Ginting, M. M., & Leslie, J. (1989). Preparation and electrical properties of heterojunctions of ZnO on  $Zn_3P_2$  and CdTe. *Can J Phys*, 67, 448-55.
- [86] Suda, T., Suzuki, M., & Kurita, S. (1983). Polycrystalline  $Zn_3P_2$  Indium-Tin Oxide Solar Cells. *Jpn J Appl Phys*, 22, L656-8.
- [87] Catalano, A. A. (1980). Evidence of p/n homojunction formation in  $Zn_3P_2$ . *Appl Phys Lett*, 37, 567.
- [88] Bhushan, M. M. (1982). Mg diffused zinc phosphide n/p junctions. *J Appl Phys*, 53, 514.
- [89] Misiewicz, J., Szatkowski, J., Mirowska, N., Jezierski, K., & Gumienny, Z. (1986). Solar energy conversion in metal-  $Zn_3P_2$  contacts. *Acta Physica Polonica*, A69, 1131-5.
- [90] Catalano, A. A. (1980). The growth of large  $Zn_3P_2$  crystals by vapor transport. *J Cryst Growth*, 49, 681-6.
- [91] Wang, Faa-Ching, Bube, R. H., Feigelson, R. S., & Route, R. K. (1981). Single crystal growth of  $Zn_3P_2$ . *J Cryst Growth*, 55, 268-72.
- [92] Deiss, J. J. L. (1988). Amorphous thin films of  $Zn_3P_2$ . *Phys Scripta*, 37, 587-92.
- [93] Murali, K. R. (1987). Properties of  $Zn_3P_2$  films grown by close space evaporation. *Materials science & engineering. A, Structural materials : properties, microstructure and processing*, 92, 193.
- [94] Soliman, M., Kashyout, A. B., Osman, M., & El-Gamal, M. (2005). Electrochemical deposition of  $Zn_3P_2$  thin film semiconductors on tin oxide substrates. *Renewable Energy*, 30, 1819-29.
- [95] Nose, Y. Y. (2012). Electrochemical Deposition of  $Zn_3P_2$  Thin Film Semiconductors Based on Potential-pH Diagram of the Zn-P- $H_2O$  System. *J Electrochem Soc*, 159, D181.
- [96] Vasekar, P. S., Adusumilli, S. P., Vanhart, D., Dhakal, T., & Desu, S. (2012). Development of zinc phosphide as a p-type absorber. *Photovoltaic Specialists Conference (PVSC), 38th IEEE*.
- [97] Adusumilli, S. P., Vasekar, P. S., Vanhart, D., Dhakal, T., Westgate, C. R., & Desu, S. (2011). Development of zinc phosphide as an absorber using chemical reflux technique. *MRS conference proceedings, Spring*.

- [98] Kimball, G. M., Müller, A., Lewis, N. S., & Atwater, H. A. (2009). Photoluminescence-based measurements of the energy gap and diffusion length of  $\text{Zn}_3\text{P}_2$ . *Appl Phys Lett*, 95, 112103.
- [99] Kimball, G. M., Lewis, N. S., & Atwater, H. A. (2010). Mg doping and alloying in  $\text{Zn}_3\text{P}_2$  heterojunction solar cells. *Photovoltaic Specialists Conference (PVSC), 35th IEEE*, 001039-43.
- [100] Wilcoxon, J. P., Newcomer, P. P., & Samara, G. A. (1996). Strong quantum confinement effects in semiconductors:  $\text{FeS}_2$  nanoclusters. *Solid State Commun*, 98, 581-5.
- [101] Altermatt, P. P., Kieseewetter, T., Ellmer, K., & Tributsch, H. (2002). Specifying targets of future research in photovoltaic devices containing pyrite ( $\text{FeS}_2$ ) by numerical modelling. *Solar Energy Mater Solar Cells*, 71, 181-95.
- [102] Chatzitheodorou, G. G. (1986). Thin photoactive  $\text{FeS}_2$  (pyrite) films. *Mater Res Bull*, 21, 1481-7.
- [103] Ennaoui, A. A. (1985). Photoactive Synthetic Polycrystalline Pyrite ( $\text{FeS}_2$ ). *J Electrochem Soc*, 132, 1579.
- [104] Ennaoui, A. (1993). Iron disulfide for solar energy conversion. *Solar Energy Mater Solar Cells*, 29, 289.
- [105] Ennaoui, A., Fiechter, S., Smestad, G., & Tributsch, H. (1990). Preparation of iron disulphide and its use for solar energy conversion. *Proceedings of 1st World Renewable Energy Congress*, 458-64.
- [106] Dahman, H. H. (1996). Iron pyrite films prepared by sulfur vapor transport. *Thin Solid Films*, 280, 56-60.
- [107] Fiechter, S. (1992). The microstructure and stoichiometry of pyrite. *J Mater Res*, 7.
- [108] Wadia, C. C. (2009). Surfactant-Assisted Hydrothermal Synthesis of Single phase Pyrite  $\text{FeS}$  Nanocrystals. *Chemistry of materials*, 21, 2568-70.
- [109] Kunst, M., & Tributsch, H. (1984). Surface microwave conductivity spectroscopy. A new experimental tool. *Chemical Physics Letters*, 105, 123-6.
- [110] Smestad, G., Da Silva, A., Tributsch, H., Fiechter, S., Kunst, M., Meziani, N., et al. (1989). Formation of semiconducting iron pyrite by spray pyrolysis. *Solar Energy Materials*, 18, 299-313.
- [111] Wu, R., Zheng, Y. F., Zhang, X. G., Sun, Y. F., Xu, J. B., & Jian, J. K. (2004). Hydrothermal synthesis and crystal structure of pyrite. *J Cryst Growth*, 266, 523-7.
- [112] Joo, J. J. (2003). Generalized and Facile Synthesis of Semiconducting Metal Sulfide Nanocrystals. *J Am Chem Soc*, 125, 11100-5.
- [113] Lin, Y. Y. Y. (2009). Extended red light harvesting in a poly(P3-hexylthiophene)/iron disulfide nanocrystal hybrid solar cell. *Nanotechnology*, 20, 405207.

- [114] Bi, Y. Y. (2011). Air Stable, Photosensitive, Phase Pure Iron Pyrite Nanocrystal Thin Films for Photovoltaic Application. *Nano letters*, 11, 4953-7.
- [115] Puthussery, J. J. (2010). Colloidal Iron Pyrite (FeS ) Nanocrystal Inks for Thin-Film Photovoltaics. *J Am Chem Soc*, 101222110759049.
- [116] Ganta, L., Dhakal, T., Rajendran, S., & Westgate, C. R. (2012). Synthesis of FeS<sub>2</sub> nanocrystals for ink-based solar cells. *MRS Online Proceedings Library*, 1447.
- [117] Dhakal, T., Ganta, L., Vanhart, D., & Westgate, C. R. (2012). Annealing of FeS<sub>2</sub> Nanocrystal Thin Film. *38th IEEE Photovoltaic Specialists Conference (PVSC)*.
- [118] Smestad, G., Ennaoui, A., Fiechter, S., Tributsch, H., Hofmann, W. K., Birkholz, M., et al. (1990). Photoactive thin film semiconducting iron pyrite prepared by sulfurization of iron oxides. *Solar Energy Materials*, 20, 149-65.
- [119] Adusumilli, S. P., & Dhakal, T. (2012). Synthesis of Iron Pyrite Film through Low Temperature Atmospheric Pressure Chemical Vapor Deposition. *MRS conference proceedings, Spring*.
- [120] Alonso-Vante, N., Chatzitheodorou, G., Fiechter, S., Mgoduka, N., Poullos, I., & Tributsch, H. (1988). Interfacial behavior of hydrogen-treated sulphur deficient pyrite (FeS<sub>2-x</sub>). *Solar Energy Materials*, 18, 9-21.
- [121] Schieck, R. R. (1990). Electrical properties of natural and synthetic pyrite (FeS<sub>2</sub>) crystals. *J Mater Res*, 5, 1567-72.
- [122] Hall, R. R. N. (1952). Electron-Hole Recombination in Germanium. *Physical review*, 87, 387.
- [123] Shockley, W. W. (1952). Statistics of the Recombinations of Holes and Electrons. *Physical review*, 87, 835-42.
- [124] Oertel, J., Ellmer, K., Bohne, W., Röhrich, J., & Tributsch, H. (1999). Growth of n-type polycrystalline pyrite (FeS<sub>2</sub>) films by metalorganic chemical vapour deposition and their electrical characterization. *J Cryst Growth*, 198-199, Part 2, 1205-10.
- [125] Ellmer, K., & Tributsch, H. (2000). Iron disulphide (pyrite) as photovoltaic material: problems and opportunities. *Proceedings of the 12th Workshop on Quantum Solar Energy Conversion*.
- [126] Alharbi, F., Bass, J., Salhi, A., Alyamani, A., Kim, H., & Miller, R. (2011). Abundant non-toxic materials for thin film solar cells: Alternative to conventional materials. *Renewable Energy*, 36(10), 2753-8.
- [127] Ramakrishna Reddy, K. T., Purandhara Reddy, P., Datta, P. K., & Miles, R. W. (2002). Formation of polycrystalline SnS layers by a two-step process. *Thin Solid Films*, 403-404, 116-9.

- [128] Devika, M., Reddy, N., & Gunasekhar, K. (2011). Structural, electrical, and optical properties of as-grown and heat treated ultra-thin SnS films. *Thin Solid Films*, 520(1), 628-32.
- [129] Devika, M., Reddy, N., Ramesh, K., Gunasekhar, K., Gopal, E., & Reddy, K. T. R. (2006). Influence of annealing on physical properties of evaporated SnS films. *Semiconductor science and technology*, 21, 1125-31.
- [130] Gunasekaran, M. M. (2007). Photovoltaic cells based on pulsed electrochemically deposited SnS and photochemically deposited CdS and  $Cd_{1-x}Zn_xS$ . *Solar Energy Mater Solar Cells*, 91, 774-8.
- [131] Avellaneda, D., Nair, M. T. S., & Nair, P. K. (2009). Photovoltaic structures using chemically deposited tin sulfide thin films. *Thin Solid Films*, 517, 2500-2.
- [132] Ramakrishna Reddy, K. T., Koteswara Reddy, N., & Miles, R. W. (2006). Photovoltaic properties of SnS based solar cells. *Solar Energy Mater Solar Cells*, 90, 3041-6.
- [133] Li, L., Liu, X., Huang, J., Cao, M., Chen, S., Shen, Y., et al. (2012). Solution-based synthesis and characterization of  $Cu_2FeSnS_4$  nanocrystals. *Mater Chem Phys*, 133, 688-91.
- [134] Yan, C., Huang, C., Yang, J., Liu, F., Liu, J., Lai, Y., et al. (2012). Synthesis and characterizations of quaternary  $Cu_2FeSnS_4$  nanocrystals. *Chem Commun*, 48, 2603-5.
- [135] Fernandes, P. P. A. (2010). A study of ternary  $Cu_2SnS_3$  and  $Cu_3SnS_4$  thin films prepared by sulfurizing stacked metal precursors. *Journal of physics.D, Applied physics*, 43, 215403.
- [136] Liu, G. G., Schulmeyer, T., Brötz, J., Klein, A., & Jaegermann, W. (2003). Interface properties and band alignment of  $Cu_2S/CdS$  thin film solar cells. *Thin Solid Films*, 431-432, 477-82.
- [137] Bragagnolo, J. A., Barnett, A., Phillips, J., Hall, R., & Rothwarf, A. (1980). The design and fabrication of thin-film  $CdS/Cu_2S$  cells of 9.15-percent conversion efficiency. *IEEE Trans Electron Devices*, 27, 645-51.
- [138] Wu, Y. Y., Wadia, C., Ma, W., Sadtler, B., & Alivisatos, A. P. (2008). Synthesis and Photovoltaic Application of Copper(I) Sulfide Nanocrystals. *Nano letters*, 8, 2551-5.